



Water dynamics in poly(vinyl pyrrolidone)–water solution before and after isothermal crystallization

S. Cervený^{a,*}, S. Ouchiar^b, G.A. Schwartz^a, A. Alegria^{a,c}, J. Colmenero^{a,c,d}

^a Centro de Física de Materiales (CSIC-UPV/EHU), Materials Physics Center, Paseo Manuel de Lardizabal 5, 20018, San Sebastián, Spain

^b Synthèses Organométalliques et Catalyse, Unite^r de Catalyse et Chimie du Solide, UMR CNRS 8181, USTL-ENSCL, Cite^r Scientifique, 59652 Villeneuve d'Ascq, France

^c Departamento de Física de Materiales, Universidad del País Vasco (UPV/EHU), Facultad de Química, Apartado 1072, 20018, San Sebastián, Spain

^d Donostia Internacional Physics Center, Paseo Manuel de Lardizabal 4, 20018, San Sebastián, Spain

ARTICLE INFO

Article history:

Received 2 October 2009

Received in revised form 26 July 2010

Accepted 4 August 2010

Available online 11 October 2010

Keywords:

Water dynamics;

Dielectric properties;

Water crystallization;

Ice;

Poly(vinyl pyrrolidone)

ABSTRACT

In this work we have studied the low-temperature dynamics of water molecules after isothermal crystallization at different temperatures (T_c) and times (t_c) of an aqueous solution of poly(vinyl pyrrolidone) (PVP) by broadband dielectric spectroscopy (BDS) and optical microscopy. Three different water concentrations ($c_w = 45, 50$ and 55 wt.%) were explored. Two major different phases were observed by optical microscopy during crystallization: one related with the core ice formed during crystallization and the other one related with the amorphous phase. Between them a rich interface was also seen. By BDS, two dielectric processes (I and II) are observed in the amorphous samples whereas, in the partially crystallized samples a third relaxation (process III) emerges in the dielectric spectra. Process II is related with the rotational dynamics of water molecules in the amorphous phase with similar characteristics to that found in the complete amorphous solutions whereas the process III is attributed to the rotation of water molecules at the interface between the ice cores and the amorphous water–PVP phase. Typical characteristics of these processes on the relaxation map are discussed.

© 2010 Elsevier B.V. All rights reserved.

1. Introduction

The behaviour of frozen aqueous solutions of polymers or sugars has been the subject of considerable study since it is involved in several fields of the food industry, biomedical technologies as well as in protocols of pharmaceuticals storage [1,2]. In spite of the fact that in all these fields it is relevant to know how molecular movements of the matrix and the water molecules are affected by freezing the solution, up to our knowledge there are no literature results concerning the dynamics of these solutions after isothermal crystallization. However, some studies related to water dynamics during non-isothermal crystallization in different solutions have been reported. For instance, the dynamics of glycerol–water solutions [3,4] was studied in a semicrystalline environment by dielectric spectroscopy. In this case, three relaxation processes were found (attributed to water–glycerol domains, interfacial water and ice). In addition, the dynamics of poly(vinyl pyrrolidone)–water solution during non-isothermal crystallization was also studied in the literature [5,6] showing a discontinuous temperature dependence of the relaxation times.

On the other hand, water dynamics in amorphous solutions of hydrophilic systems in the low-temperature range of 130–250 K have been previously investigated by dielectric spectroscopy [5–10]. From

these studies, it is well-known that a relaxation process associated with the reorientation of the water molecules in the solution is observed (the so-called Process II in references [7–10]). The temperature dependence of the relaxation times are usually Arrhenius-like below the glass transition temperature (T_g) of the solution, suggesting that in this temperature range water motions are restricted by the glassy matrix. In addition, at temperatures higher than T_g , a systematic deviation of the Arrhenius behaviour is observed and attributed to the fact that water molecules can move in an unhindered or unobstructed medium [5–10].

In this work we address the behaviour of water dynamics after isothermal crystallization i.e. in a semicrystalline environment. To do that, we analyze the water dynamics before and after isothermal crystallization at different crystallization temperatures (T_c) and crystallization times (t_c) in samples of poly(vinyl pyrrolidone)–water solutions (water concentration, $c_w = 45, 50$ and 55 wt.%). As the response of water molecules in this amorphous material is well-characterized [5], we are able to compare the dielectric response of water molecules in a partially crystallized environment with that in the amorphous material and to discuss how the water dynamics is affected by crystallization.

2. Experimental

Poly(vinyl pyrrolidone) (PVP) in aqueous solution at a water concentration of $c_w = 55$ wt.%, was purchased from Aldrich Chemical

* Corresponding author. Tel.: +34 943018808; fax: +34 943015800.

E-mail address: scervený@ehu.es (S. Cervený).

and was used without any further purification. The weight-average molecular weight M_w of the dry polymer is 160,000 g/mol. Different water concentrations were reached by evaporating water from the sample as received under normal room conditions. In this way, additional samples with $c_w = 50$ and 45 wt.% were obtained.

Optical microscopy measurements were performed using a LEICA 5500DM equipped with a Linkam heating-cooling stage. The images were obtained and processed with a Leica Image Processing software.

A broadband dielectric spectrometer, Novocontrol Alpha analyzer, was used to measure the complex dielectric function $\epsilon^*(\omega) = \epsilon'(\omega) - i\epsilon''(\omega)$, $\omega = 2\pi f$, in the frequency (f) range from $f = 10^0$ Hz to $f = 10^7$ Hz. In this way each spectrum was collected in a time that does not exceed 1 min. The samples were placed between parallel gold-plated electrodes with a diameter of 30 mm and thickness of 0.1 mm (Teflon spacer). The sample temperature was controlled with stability better than 0.1 K. In this work, the dielectric response was described by using a sum of empirical Cole–Cole functions [11]

$$\epsilon^*(\omega, t_c) = \epsilon_\infty + \sum_j \frac{\Delta\epsilon_j}{[1 + (i\omega\tau_j)^\alpha]^j} \quad (1)$$

where $\Delta\epsilon_j = \epsilon_s - \epsilon_\infty$, with ϵ_∞ and ϵ_s being the un-relaxed and relaxed values of the dielectric constant, τ_j as the characteristic relaxation time and α as the shape parameter ($0 < \alpha \leq 1$) which describe the symmetric broadening of the relaxation. As we will show in the next section, we chose two or three CC functions to describe the dielectric spectra of amorphous and semicrystalline samples respectively.

Finally, differential scanning calorimeter (DSC) measurements were made by using a Q2000 TA Instrument.

3. Results and discussion

3.1. Calorimetric response

A typical DSC scan showing the heat flow of PVP–water solution with $c_w = 55$ wt.% during cooling and heating (at a rate of 10 K/min) is given in Fig. 1. It is evident that it is possible to avoid crystallization on cooling obtaining a glass phase at low temperatures. However, the heating scan in Fig. 1 shows a glass transition ($T_{g,onset} = 205$ K) followed by a cold crystallization in the temperature range of 230–250 K. After that, a broad melting is observed in the temperature range between 250 and 270 K. The T_g of all the samples was

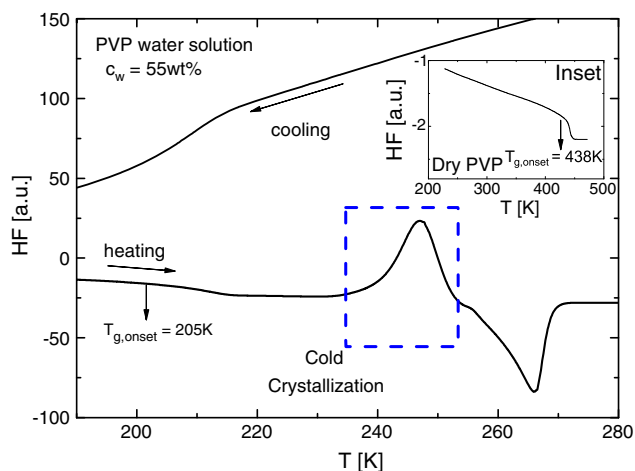


Fig. 1. Heat flow measured by DSC during cooling and heating at a rate of 10 K/min of PVP–water solution with $c_w = 55$ wt.%. A cold crystallization is observed in the temperature range of 230–255 K (dotted box). $T_{g,onset}$ represents the onset of the glass transition temperature (T_g). Inset: DSC scans of dry PVP where no crystallization is observed.

determined as the onset of the heat flow step. The inset of Fig. 1 shows the calorimetric response of dry PVP. In this case, no crystallization at all is observed and consequently the only component in this mixture that presents crystallization is the water. Therefore in this work we are dealing with the behaviour of water molecules during the crystallization of water itself.

3.2. Optical microscopy

In order to analyze both the ice morphologies and the crystallization kinetics, optical microscopy measurements were performed (magnification 20 \times). The samples were quickly cooled at a rate of 40 C/min down to 170 K. After that, the samples were heated again up to the desired crystallization temperature (T_c) and were held (during t_c) to observe the behaviour during crystallization. Spherulitic-like structures with very similar morphologies were observed for all water concentration and temperatures explored. Fig. 2 shows the evolution of the ice cores formed during isothermal crystallization. At $t_c \approx 10$ min, small spherulitic-like structures of ice (opaque) appear in the samples and an increment in the diameter with crystallization

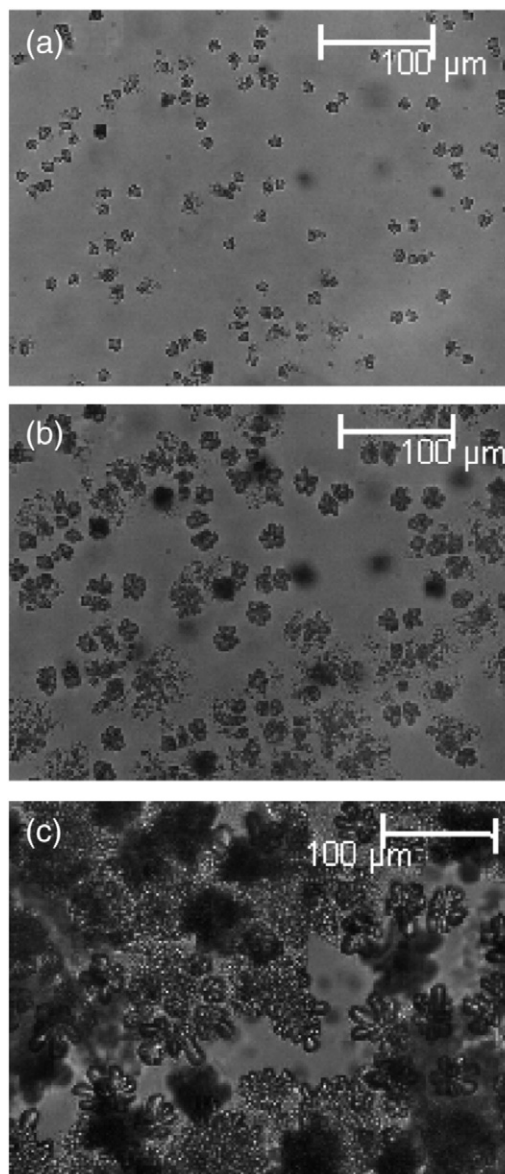


Fig. 2. Evolution of ice diameter during crystallization at $T_c = 215.15$ K and $t_c = 12$, 70 and 348 min respectively for a solution with $c_w = 55$ wt.%.

time is noted. After approximately 200 min, two different and stable phases are clearly observed. The clear (transparent) phase corresponds to the amorphous state of PVP–water solution. It is expected that the final water concentration of this PVP-rich phase changes during crystallization. We have to mention that after 200 min (depending on T_c and water concentration) there is no macroscopic evolution of the images as seen in the micrographs. However, as we will discuss in the later part, the dielectric response still changes at longer crystallization times.

By measuring the diameter of ice crystals during isothermal crystallization at different times, it is possible to construct the plot shown in Fig. 3 to analyze the influence of the super-cooling degree. At T_c higher than 240 K (low degree of super-cooling) the crystallization proceeds very fast and it is not possible to observe the full amorphous material at $t_c = 0$ min. However, at high degree of super-cooling ($T_c < 240$ K) the slow nucleation rate allows us to observe the completely amorphous material and then permits us to follow the growing of the spherulitic-like structures of ice. For this reason we chose to measure the dielectric response at a high degree of super-cooling ($T_c < 240$ K) in order to have enough time for recording the dielectric response of the completely amorphous samples. Finally, we note that the slope in Fig. 3 changes with time indicating a change in the final water concentration of PVP-rich phase.

3.3. Procedure of crystallization for dielectric measurements

First of all the dielectric spectra of the completely amorphous sample were measured in the temperature range from constant 150 to 220 K (step 1). After that, the temperature (T_c) was maintained during some time (t_c) while the dielectric spectra was acquired isothermally every 1 min (step 2). Next to this procedure, the sample was cooled to 150 K, and the dielectric spectra were measured every 5° in the temperature interval from 150 K to 220 K (step 3). Finally the sample was heated at 280 K, melted for 1 min and immediately cooled again at a different T_c in order to let the amorphous sample crystallize during another time interval. In this way we can monitor the dielectric response of the amorphous sample (step 1), the dielectric response after crystallization (step 3) as well as the dielectric response during isothermal crystallization (step 2) which will not be discussed in this work. We chose three crystallization temperatures ($T_c = 215.15$, 219.15 and 221.15 K) whereas for each temperature the crystallization times were $t_c = 30, 60, 150, 180, 360$, and 570 min, respectively. Note that this procedure was successfully applied for crystalline polymers and widely discussed in the literature [12–14].

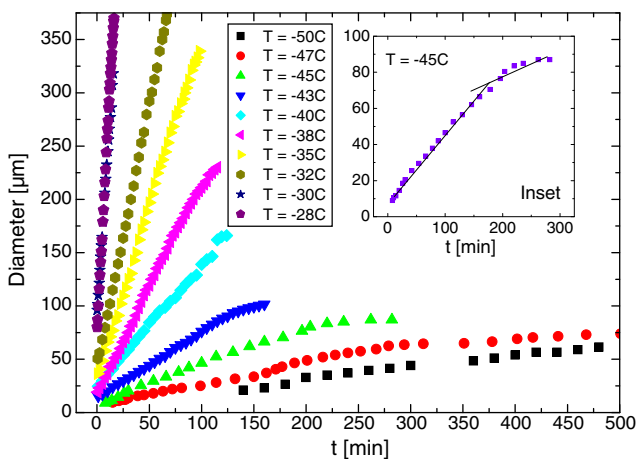


Fig. 3. Diameter of ice crystal as a function of the time at different crystallization temperatures for a PVP–water solution with $c_w = 55$ wt.%. Inset: Diameter of ice crystal as a function of time at $T_c = -45$ °C.

3.4. Water dynamics in the amorphous state—dielectric response

Isothermal data of the dielectric loss ϵ'' of amorphous PVP–water mixtures are shown in Fig. 4a at different temperatures. Here, we summarize the main results concerning the water dynamics in amorphous PVP–water mixtures previously studied in Reference [7]. The dielectric response of these amorphous mixtures shows a prominent peak due to the reorientation of water molecules (process II in Fig. 4a). In addition, a faster and weak process is also observed (process I in Fig. 4a). Thus, the response of the amorphous samples was described by using two Cole–Cole functions [11] each one related with the previously mentioned processes.

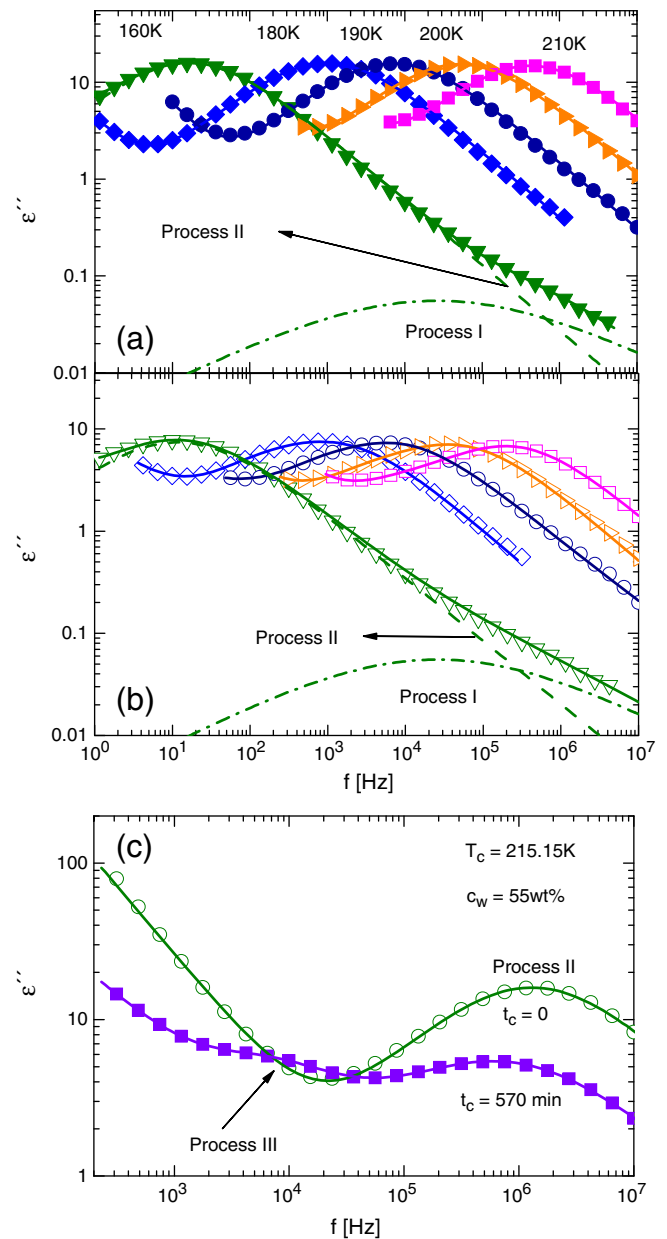


Fig. 4. (a) Loss component, ϵ'' , of the complex permittivity, $\epsilon^*(f)$, of amorphous PVP–water solution with $c_w = 55$ wt.% at different temperatures. The lines through the data points correspond to least-squares fits to a superposition of two Cole–Cole functions. (b) Same than in subpanel (a) after isothermal crystallization at $T_c = 215.15$ K during $t_c = 390$ min. The solid lines through the data points correspond to least-squares fits to a superposition of three Cole–Cole functions (process III cannot be well observed in this representation) (c) Loss component, ϵ'' , of the complex permittivity, $\epsilon^*(f)$, of the amorphous sample ($t_c = 0$) and after isothermal crystallization during 570 min. The new small process (process III) at low frequencies can be observed.

The temperature dependence of the corresponding relaxation times is shown in Fig. 5a (filled symbols) where the two processes (I and II) can be observed. Process II shows a crossover from high temperature non-Arrhenius to low-temperature Arrhenius behaviour at certain temperature, T_{cross} , close to the calorimetric $T_{g,\text{DSC}}$. We have associated the presence of this crossover with the appearance of finite size effects affecting water dynamics when the whole system becomes frozen [7–9]. In other words, at temperatures lower than T_g the molecular movements of the system as a whole are frozen and therefore the water dynamics occurs in a restricted environment. In this way, the low temperature water dynamics ($T < T_g$) has the characteristic of a secondary relaxation (symmetric relaxation and the temperature dependence of the relaxation times is Arrhenius-like). However, at higher temperatures ($T > T_g$) the whole system can move and consequently the water dynamics is highly cooperatively-like. Thus in this temperature range the relaxation times follow a non-Arrhenius temperature dependence.

Process I has an activation energy of 0.24 eV and remains Arrhenius over the whole temperature interval analyzed. In the next section, we compare these typical characteristics of water dynamics in amorphous PVP–water solutions with the results obtained for the water dynamics after isothermal crystallization.

3.5. Water dynamics in a semicrystalline state (after isothermal crystallization)

Fig. 4b shows an example of the dielectric spectra obtained for a sample with $c_w = 55$ wt.% after isothermal crystallization during

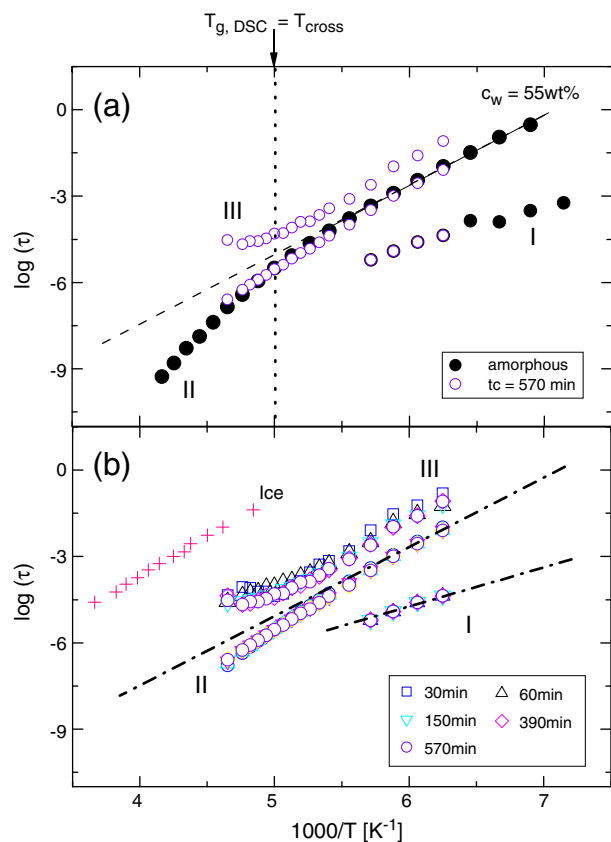


Fig. 5. (a) Temperature dependence of the relaxation times of both amorphous PVP–water mixtures (full symbols) and after isothermal crystallization during $t_c = 570$ min at $T_c = 215.15$ K (open symbols). (b) Temperature dependence of the relaxation times for partially crystallized samples at different times (t_c). The crosses show the experimental results for bulk ice taken from Reference [15] and the dash-dot lines represent the relaxation time of the amorphous sample shown in subpanel (a).

$t_c = 570$ min at $T_c = 215.15$ K. Similar results were obtained for the other water concentrations, T_c and t_c . Clearly, the intensity of the dielectric loss is smaller in the semicrystalline mixture (Fig. 4b) than in the amorphous solution (Fig. 4a) since part of the amorphous water turns into ice and therefore does not contribute to the dielectric signal. In addition, the presence of a new process (not well resolved in the scale of Fig. 4b) at lower frequencies is observed (see Fig. 4c, at frequencies of about 10^4 Hz). This new process appears for all T_c and t_c explored as well as for all the different c_w analyzed. Therefore, to fit the dielectric response after crystallization, we have used a sum of three Cole–Cole functions, two of them for taking into account the processes also observed in the amorphous samples (processes I and II) and the other one, related to the new process at low frequencies (process III). Fig. 4(b and c) show the results of this fitting in solid lines. As we show in the later part, the new relaxation process which appears in the semicrystalline samples is most likely related with the reorientation of water molecules at the interface between the ice phase and the amorphous material.

Fig. 5a shows the temperature dependence of the relaxation time obtained from the fits of a sample crystallized during $t_c = 570$ min at $T_c = 221.15$ K (open symbols). The temperature dependence of the relaxation time corresponding to processes I and II are similar to the amorphous sample (filled symbols in Fig. 5a). In addition, the main process (process II) presents a crossover from non-Arrhenius to Arrhenius behaviour as in the case of the amorphous sample at T_g . However, the crossover temperature (T_{cross}) progressively shifts to higher temperatures which could be a consequence of the fact that the remaining amorphous phase is continuously changing the water concentration during crystallization and therefore also the glass transition temperature gradually moves to higher temperature (note that the water molecules in the amorphous phase turned into ice during crystallization and this fact changes the water concentration in the amorphous phase). At low temperatures ($T < 180$ K), the temperature dependence of the relaxation time of process II can be described by the Arrhenius law, $\tau = \tau_0 \exp(E_a/kT)$ with $E_a = 0.54$ eV, as shown in Fig. 5b in dash-dot line. Note that this energy value was found to be universal for water in several hydrophilic solutions [8] and it is still valid for partially crystallized samples.

Another characteristic of the dynamics in the samples isothermally crystallized is that their relaxation times are independent of the crystallization time at temperatures lower than T_g as observed in Fig. 5b. Fig. 6(a and b) shows the dielectric response at two temperatures $T = 180$ K (lower than T_g) and $T = 215$ K (higher than T_g) for different crystallization times ($t = 0$ min represents the amorphous sample). Clearly, at $T = 180$ K the relaxation time in the amorphous and semicrystalline materials are the same for all the crystallization times analyzed although the dielectric intensity decreases since water molecules turned into ice. However, at $T = 215$ K, the main loss peak in the semicrystalline material shifts continuously toward lower frequencies for more than half a decade (see Fig. 6b). From this observation, we can conclude that at temperatures lower than T_g the relaxation due to water molecules (process II) is independent of the environment being only related with the fact that water molecules are confined by a matrix (this matrix could be the frozen polymer or the ice phase). This also implies that process II is a rather local process.

Finally, we focus on the new slow process observed in the partially crystallized samples (process III). The temperature dependence of the relaxation time of this behavior process also presents a crossover from non-Arrhenius to Arrhenius (see Fig. 5a and b). The activation energy at low temperatures (Arrhenius behaviour) is about 0.46 eV. The rotation of water molecules within the ice crystals or the rotation of water molecules at the interface between the ice crystals and the amorphous material could be both the origin of this relaxation. In order to investigate these hypotheses we compared our relaxation results with the dielectric response of bulk ice measured by Auty and

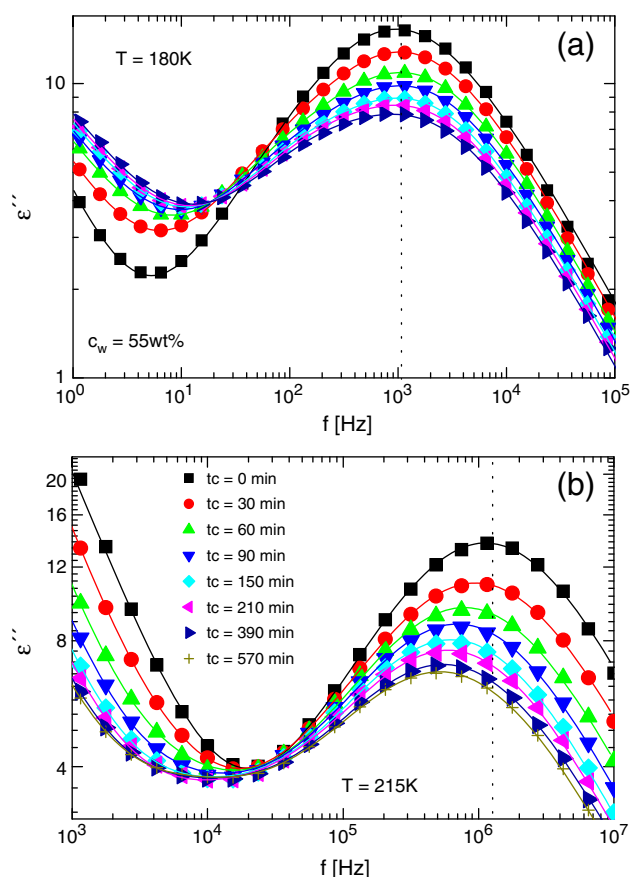


Fig. 6. Loss component, ϵ'' , of the complex permittivity, $\epsilon^*(f)$, of amorphous PVP–water solutions (black boxes) and after isothermal crystallization at $T_c = 215.15$ K at different times (0, 20, 60, 90, 150, 210, 390 and 570 min respectively) at two temperatures (a) $T = 180$ K and (b) $T = 215$ K. Curves at $t = 0$ min (black boxes) represent the response of the amorphous material whereas the rest of the curves represent the dynamics after crystallization at different times (t_c).

Cole [15]. The temperature dependence of the relaxation time corresponding to ice is shown in Fig. 5b (crosses). The activation energy for ice is about 0.64 eV, much higher than that corresponding with process III (0.46 eV) in the Arrhenius part. Consequently, we could relate this process with the presence of interfacial water between the ice regions and the water–PVP amorphous phase. Although this interpretation is in agreement with that by Hayashi

et al. in glycerol–water mixtures [3], more studies are necessary to establish this correspondence.

4. Conclusion

We have analyzed the dynamics of water molecules before and after isothermal crystallization in PVP–water mixtures. Three dielectric processes (namely processes I, II and III) were found in the semicrystalline samples, two of them also present in the amorphous samples (processes I and II). Whereas process II is related with the rotational dynamics of water molecules in the amorphous phase, process III can be related with the rotation of water molecules at the interface between the amorphous phase and the ice phase respectively. The relaxation time corresponding to process II in the semicrystalline samples is independent of the crystallization level (i.e. independent of the crystallization time) at temperatures lower than T_g , when water molecules are confined by the glassy matrix formed by both the glassy polymer and the ice regions.

Acknowledgements

The authors gratefully acknowledge the support of the Spanish Ministry of Science and Innovation, project CSD2006-00053 and MAT2007-63681; the European Union, project 502235-2 and the Basque Government, and project IT-436-07.

References

- [1] E.Y. Shalaev, T.D. Johnson-Elton, L.Q. Chang, M.J. Pikal, *Pharm. Res.* 19 (2002) 195.
- [2] S.A. Barker, R. He, D.Q.M. Craig, *J. Pharm. Sci.* 90 (2001) 157.
- [3] Y. Hayashi, A. Puzenko, I. Balin, Y.E. Ryabov, J. Feldman, *J. Phys. Chem. B* 109 (2005) 9174.
- [4] Y. Hayashi, A. Puzenko, J. Feldman, *J. Phys. Chem. B* 109 (2005) 16979.
- [5] S. Yagihara, M. Asano, M. Kosuge, S. Tsubotani, D. Imoto, N. Shinyashiki, *J. Non-Cryst. Solids* 351 (2005) 2629.
- [6] S. Sudo, M. Shimomura, N. Shinyashiki, S. Yagihara, *J. Non-Cryst. Solids* 307–310 (2002) 3565.
- [7] S. Cerveny, A. Alegría, J. Colmenero, *J. Chem. Phys.* 128 (2008) 044901.
- [8] S. Cerveny, A. Alegría, J. Colmenero, *Phys. Rev. E* 77 (2008) 031803.
- [9] S. Cerveny, J. Colmenero, A. Alegría, *Eur. Phys. J. Spec. Top.* 141 (2007) 49.
- [10] S. Cerveny, J. Colmenero, A. Alegría, *J. Non-Cryst. Solids* 353 (2007) 4523.
- [11] R.H. Cole, K.S. Cole, *J. Chem. Phys.* 10 (1942) 98.
- [12] M. Soccio, A. Nogales, N. Lotti, A. Munari, T.A. Ezquerra, *Phys. Rev. Lett.* 98 (2007) 037801.
- [13] A.R. Bras, M.T. Viciosa, Y. Wang, M. Dionisio, J.F. Mano, *Macromolecules* 39 (2006) 6513.
- [14] S. Cerveny, P. Zinck, M. Terrier, S. Arrese-Igor, A. Alegría, J. Colmenero, *Macromolecules* 41 (2008) 8669.
- [15] R.P. Auty, R.H. Cole, *J. Chem. Phys.* 20 (1952) 1309.